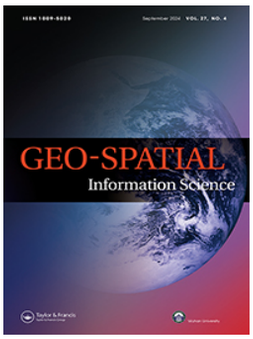

Geo-spatial Information Science

ISSN: (Print) (Online) Journal homepage: www.tandfonline.com/journals/tgsi20

Untangling the association between urban mobility and urban elements

Jinzhou Cao, Wei Tu, Rui Cao, Qili Gao, Guanzhou Chen & Qingquan Li

To cite this article: Jinzhou Cao, Wei Tu, Rui Cao, Qili Gao, Guanzhou Chen & Qingquan Li (2024) Untangling the association between urban mobility and urban elements, Geo-spatial Information Science, 27:4, 1071-1089, DOI: 10.1080/10095020.2022.2157761

To link to this article: https://doi.org/10.1080/10095020.2022.2157761

© 2023 Wuhan University. Published by Informa UK Limited, trading as Taylor & Francis Group.

Published online: 15 Feb 2023.

Submit your article to this journal

Article views: 1891

View related articles

View Crossmark data

Citing articles: 4 View citing articles

Full Terms & Conditions of access and use can be found at
https://www.tandfonline.com/action/journalInformation?journalCode=tgsi20

GEO-SPATIAL INFORMATION SCIENCE
2024, VOL. 27, NO. 4, 1071–1089
https://doi.org/10.1080/10095020.2022.2157761

Taylor & Francis
Taylor & Francis Group

OPEN ACCESS Check for updates

Untangling the association between urban mobility and urban elements

Jinzhou Cao [a,b], Wei Tu [c], Rui Cao [d], Qili Gao [c], Guanzhou Chen [e] and Qingquan Li [c]

[a]College of Big Data and Internet, Shenzhen Technology University, Shenzhen, China; [b]Key Laboratory of National Geographic Census and Monitoring, Ministry of Natural Resources, Wuhan University, Wuhan, China; [c]School of Architecture and Urban Planning & Guangdong Key Laboratory of Urban Informatics, Shenzhen University, Shenzhen, China; [d]Department of Land Surveying and Geo-Informatics & Smart Cities Research Institute, The Hong Kong Polytechnic University, Hong Kong, China; [e]State Key Laboratory of Information Engineering in Surveying Mapping and Remote Sensing, Wuhan University, Wuhan, China

ABSTRACT

Understanding complex urban systems necessitates untangling the relationships between diverse urban elements such as population, infrastructure, and socioeconomic activities. Scaling laws are basic but effective rules for evaluating a city's internal growth logic and assessing its efficiency by investigating whether urban indicators scale with population. To date, only limited research has empirically explored the scaling relations between variables of urban mobility in mega-cities at an intra-urban scale of a few meters. Using multiple urban-sensed and human-sensed data, this study proposes a thorough framework for quantifying the scaling laws in a city. To begin, urban mobility networks are built by aggregating population flows using large-scale mobile phone tracking data. To demonstrate the spatiotemporal variability of urban mobility, various network-based mobility measures are proposed. Following that, three different features of urban mobility laws are exposed, explaining spatial agglomeration, spatial hierarchical structures, and the temporal growth process. The scaling correlations between urban indicators pertaining to socioeconomic features and infrastructure and a mobility-population measure are then quantified using multi-sourced urban-sensed data. Applying this framework to the case study of Shenzhen, China revealed (a) spatial travel heterogeneity, hierarchical spatial structures, and mobility growth, and (b) not only a robust sub-linear relationship between infrastructure volume and population, but also a sub-linear relationship for socioeconomic activity. The identified scaling laws, both in terms of mobility measures and urban indicators, provide a multi-faceted portrait of the spatio-temporal variations of urban settings, allowing us to better understand intra-urban developments and, consequently, provide critical policy evaluations and suggestions for improving intra-urban efficiency in the future.

ARTICLE HISTORY
Received 24 December 2021
Accepted 7 December 2022

KEYWORDS
Scaling law; urban scaling; urban mobility; intra-urban system; mobile phone data

1. Introduction

Cities are typical complex systems in which numerous urban features such as people, infrastructure, and socioeconomic activity interact in sophisticated ways (Tu et al. 2017; Chong et al. 2018). Globally, increased urbanization has resulted in rapid growth of the city-dwelling population (Tu et al. 2020). Cities now attract more than half of the worldwide population, produce at least 80% of the money, and drive more than 90% of the reformation (Batty 2008). This explosive population growth has supported socioeconomic development and infrastructure renewal while also bringing urban challenges such as traffic congestion, environment pollution, and reduction in quality of life (Cavoli 2021). To gain a greater understanding of these urban features, a new perspective is sought that can quantitatively characterize their interconnected relationships.

Scaling laws are useful yet basic guidelines that aid in the comprehension of urban features (Brockmann, Hufnagel, and Geisel 2006). They reveal significant patterns between two explainable urban indicators in the power-law-like regime $Y \sim P^{\beta}$, where β is the scaling exponent (Arcaute et al. 2015). The indicators in turn reveal the geographical arrangements of urban features such as population, infrastructure, and socioeconomic activity. For instance, the population agglomeration in cities produces scale effects, which suggests that the economic production of a city with population one million is larger than the total outputs of two cities with population 0.5 million, yet the former consumes fewer resources and requires less infrastructure per capita (Ribeiro et al. 2021). Therefore, scaling laws, which characterize the non-linear patterns that relate to these urban indicators, can describe a city's internal growth logic and agglomeration law.

However, previous studies have regarded many cities as unitary entities and explored macroscopic scaling properties across a region or country. These studies represent the condition and nature of whole urban systems, leaving much room for micro-scale heterogeneity among regions within a city. Current

CONTACT Wei Tu tuwei@szu.edu.cn

© 2023 Wuhan University. Published by Informa UK Limited, trading as Taylor & Francis Group.
This is an Open Access article distributed under the terms of the Creative Commons Attribution License (http://creativecommons.org/licenses/by/4.0/), which permits unrestricted use, distribution, and reproduction in any medium, provided the original work is properly cited. The terms on which this article has been published allow the posting of the Accepted Manuscript in a repository by the author(s) or with their consent.

urban planning and resource allocation pay attention to fine-grained spatial planning, which requires an understanding of the coupling relationship between urban elements and human mobility at a small scale. Performing analysis at this fine scale aids us in verifying and comprehending the consistency in and contrasts between current urban regulations at various scales. In practice, micro-scale urban studies are based on the daily living units of the populace, such as streets, neighborhoods, 15-minute living circles, and business districts. In addition, there are differences in the characteristics of geographical arrangements at multiple scales, leading to valid arguments about whether many existing macro-scale laws can be effectively extended to the micro-scale, such as whether the scale effect of a city's economic production also exists at the micro-scale. Scaling laws have been claimed in the intra-urban system (Dong et al. 2020; Liang et al. 2013), but investigation at fine scale remains largely unaddressed, despite it representing a crucial urban development perspective.

Urban mobility investigates urban features as well as the underlying patterns that underpin intra- and inter-urban movements (Tu et al. 2018; Maeda et al. 2019); therefore, it captures genuine population flows and regional interconnections between intra-urban areas (Diao, Kong, and Zhao 2021). As a consequence, intra-urban mobility properties are good proxies for the population sizes of small areas (Yin and Chi 2021). More crucially, features related to intra-urban mobility have been observed to follow scaling laws (Wang et al. 2015; Cao et al. 2019). However, the scaling laws between urban mobility variables have yet to be thoroughly elucidated. Urban mobility is represented by a characteristic network structure, and inherent network properties enable the use of intra-urban network indicators inside a city to investigate intra-urban mobility scaling laws. Furthermore, urban mobility patterns are highly dynamic, and the temporal dynamics of scaling processes yield valuable clues into the evolution of urban systems. Thus, in order to acquire a complete knowledge of urban systems and measure a city's performance, it is also essential to assess scaling laws linked to mobility indicators.

This study developed a comprehensive framework for quantifying intra-urban mobility scaling laws in terms of both the meter-level urban indicators and mobility indicators. Using Shenzhen, the typical Chinese mega-city, as the research area, we first partitioned the urban region into a high-resolution spatial grid. We subsequently built urban mobility networks by combining the entire area's averaged population movements obtained from large-scale mobile phone location data. To explain the spatio-temporal heterogeneity of urban mobility, we introduced network-oriented mobility measures such as area connectivity, area popularity, neighborhood interaction, and mobility growth rate. We discovered three different aspects of urban mobility laws that describe spatial agglomeration, spatial hierarchical structures, and the divergent temporal growth process in the city as a whole and at grid level. We also identified socioeconomic and infrastructure-related urban indicators and quantified their scaling relationships with the derived grid-level population, which is a better proxy for high-resolution population. The super-linear scaling laws between infrastructure volume and population and sub-linear scaling laws for socioeconomic activity were verified on the mesoscopic scale. Additionally, we found the scaling laws to have obvious heterogeneity within the city. The discovered scaling laws present a multi-faceted portrayal of urban development in the context of mobility measures and urban indicators alike, providing vital implications for data-informed urban policy and development.

This study makes the following contributions. First, it discovers urban scaling laws at the meter scale. It differs from previous studies that focused on macro-scale scaling between cities while ignoring varying intra-urban distributions. These insights help policy-makers in assessing the urban development condition. Second, it presents a methodology for unraveling intra-urban scaling laws from the standpoint of dynamic urban mobility with very simple and easy-to-understand formulas and using easy-to-obtain data. Third, the findings of this study contribute to a better understanding of the spatial-temporal evolution of urban mobility patterns. In light of trends in urban growth, these findings are complementary to urban studies in a diverse but typical urban setting.

The rest of this paper is structured as follows: Section 2 reviews the related work. Section 3 introduces the methodology for performing urban and mobility scaling law analyses. Section 4 introduces the study area and data sources, as well as summarizes the findings and explains the scaling properties that were discovered. Section 5 finally discusses conclusions and future work.

2. Related work

2.1. Scaling laws in urban contexts

Scaling laws are among the fundamental laws and mechanisms that underpin complex systems in fields such as biology, physics, and network science (Bettencourt 2013; Bettencourt et al. 2007). Kleiber's Law, for example, claims that the metabolic rate and body weight of adult animals follow a 3/4 power-law relationship (Kleiber 1947). Significant progress has been made in our understanding of scaling laws in urban environments, often by studying whether various urban indicators scale with population size within

an urban system (Xu et al. 2019; Meirelles et al. 2018; Lei et al. 2021). An urban scaling law reflects the state and characteristics of the urban system rather than the characteristics of individual cities, and the validity of scaling laws has been thoroughly established in many different urban systems (Rybski, Arcaute, and Batty 2019; Bettencourt, Lobo, and Youn 2013; Giometto et al. 2013). Moreover, urban scaling laws have been examined in cities all over the world, including in Europe (Bettencourt and Lobo 2016), India (Sahasranaman and Bettencourt 2019), China (Zünd and Bettencourt 2019), and other countries besides, and solid laws have been elucidated, such as a sub-linear scaling between land area and population size that applied in European cities from 1280 to 1320 (Cesaretti et al. 2016). This clearly shows that the urban scaling law is a universal norm in urban systems that is unaffected by history, geography, or culture.

The urban scaling law is typically expressed as the power function $Y = Y_0 P^{\beta}$, where Y is an urban indicator, P is the population size, and β is referred to as the scaling exponent. The scaling relationship is quantitatively reflected in the magnitude of the exponent (Rybski, Arcaute, and Batty 2019), and urban indicators may be classified into three types depending on exponent magnitude: (1) For socioeconomic factors (such as Gross Domestic Product [GDP], knowledge output, serious violent crime, and so on), of economically and culturally diverse, nations empirical evidence suggests that the scaling exponent should be more than one (usually approximately $\beta = 1.15$ (Meirelles et al. 2018)) and the size of the urban population rises super-linearly. This is due to the effect of increased returns to scale, which causes social interaction to rise super-linearly with population growth. (2) For infrastructure indicators (such as road length, number of gas stations, etc.), empirical results show that the scaling exponent should be around 0.85 (Kühnert, Helbing, and West 2006). This means that larger cities require less infrastructure per capita (Norman, MacLean, and Kennedy 2006), allowing us to state that larger cities accomplish more with less, reflecting the economies of scale (Bettencourt and West 2011; Meirelles et al. 2021). (3) Urban indicators connected to individual demands of urban inhabitants (such as the number of employers, household water usage, and so on) usually have an exponent equal to one, and the size of the urban population changes linearly with this type of indicator (Bettencourt et al. 2007).

The term "urban system" can refer to either a city itself or an urban system made up of many cities (Berry 1964). Most existing research has regarded each targeted city as a whole and investigated inter-urban scaling properties across a region or a country. Hence, the intra-urban variation within a city is largely understudied. Differences in the characteristics of geographical arrangements are evident in different urban areas, which calls into question whether many existing inter-urban laws can be effectively extended to smaller scales, for example whether the scale effects of a city's economic production exist within that city. Recent studies support that scaling laws exist in the intra-urban system, which is comprised of districts or communities (Dong et al. 2020; Liang et al. 2013), but the narrow intra-urban scale of a few meters remains little understood, despite the benefits of such understanding to more refined urban research and urban planning.

2.2. Scaling laws in urban mobility

Urban mobility analysis is a fundamental topic of study in the interdisciplinary field, including transport, urban planning, and geographic informatics, focusing on the spatio-temporal features as well as hidden patterns behind intra-urban and inter-urban movements (Xu et al. 2018; Gallotti and Barthelemy 2014). Urban mobility properties reflect fluctuation in the desirability of regions within a city as humans travel (Cao et al. 2021). In addition, the idea of urban mobility is comprehensive of human travels at both individual and group levels, which supports ramifications such as pandemic prevention (Zhou et al. 2020), migratory flow prediction (Huang et al. 2018), urban planning (Bokányi, Kallus, and Gódor 2019), and location-based services (D'Silva et al. 2018).

In the context of urban mobility analysis, scaling laws are thought to be particularly helpful in obtaining a qualitative description of global character. According to prior studies, indicators associated with urban mobility exhibit scaling properties (Wang et al. 2015; Cao et al. 2019). For example, the experimentally observed universal law of distance – frequency scaling of flows to individual places fits Zipf's law for trip distance (Yan et al. 2013) and visiting frequency distributions (Schläpfer et al. 2021; Zheng and Zhou 2017). This Zipf's law states that people optimize the distance and frequency of their visits.

Urban mobility may be represented by a specific network structure, and hence intrinsic network qualities allow for the use of intra-urban network indicators inside a city to examine intra-urban mobility scaling (Becker et al. 2013). Complex network theory, which provides tools for describing network topology and spatial patterns and gives quantitative measurements such as node degree, node strength, and clustering coefficients (Albert and Barabási 2002), has recently inspired such study using urban mobility data (Guidotti et al. 2016). However, there is yet a major lack of research exposing the scaling laws between these intricate network-based indicators. Additionally, urban mobility patterns are very dynamic, and the temporal dynamics of scaling

processes provide vital insights into evolution of the system. Therefore, it is necessary to examine scaling laws associated with mobility indicators in order to achieve a thorough understanding of urban systems and quantify a city's efficiency.

2.3. Urban big data analytics

With the advent of the big data era, the mobile Internet, and a large number of intelligent terminal devices, accurate, real-time spatio-temporal data can be generated that is centered on urban layouts as well as individual residents, which completely compensates for traditional data shortcomings such as difficulty in obtaining data, small data volume, time lag, and partially static data (Thatcher, Shears, and Eckert 2018). This trend has far-reaching implications for urban analysis, particularly for the study of urban scaling laws. Urban spatial data, such as Point of Interest (POI) data, building data, road network data, and so on, have shown exceptional potential for describing a city's state through the computation of urban indicators (Liu et al. 2018). For example, by utilizing building vector data, academics may discover urban functions and obtain a deeper knowledge of urban structures (Niu et al. 2017). Road network data contains essential transport properties, allowing the investigation of geographical variances in infrastructure development (Strano et al. 2017). POI data demonstrates the distribution of urban facilities. Collectively, these fundamental spatial data sources offer a fresh viewpoint on urban indicators.

Mobile phone positioning data, vehicle GPS sequences, smart card records, and social media check-in data are examples of data sources that may be used to trace individual trajectories and infer urban mobility patterns. Mobile phone location data in particular has garnered scholarly interest in the recent decade (Blondel, Decuyper, and Krings 2015; Calabrese et al. 2011; Cao et al. 2021) due to its high penetration rate, large data volume, high currency, and low cost. By aggregating the trips of large populations extracted from mobile phone data, features of urban mobility can be analyzed; for example, Louail et al. (2015) highlighted the spatial structure of commuting networks retrieved from mobile phone data. Accordingly, phone location data has been extensively utilized in urban mobility research in order to develop better knowledge of both individual travel behaviors and collective mobility patterns. This knowledge emphasizes the characterization of urban mobility and can be used to better explain human behaviors and urban structures, including transport inequality (Zhou, Yeh, and Yue 2018), activity space (Gao et al. 2021), social interaction (Calabrese et al. 2011), urban hot spots (Hoteit et al. 2014), population distribution (Deville et al. 2014), and land use (Tu et al. 2017).

While such studies levering big data have offered considerable insight into urban dynamics, there remains need for comprehensive investigations of scaling laws in this age of big data. In this study, we will synthesize data from diverse sources to construct typical urban and mobility indicators, as well as analyze intra-urban scaling laws. As such, this study addresses gaps left by earlier research and expands our understanding of cities.

3. Materials and methods

3.1. Framework

This research proposes a comprehensive framework for quantifying intra-urban mobility scaling laws in terms of both meter-level urban indicators and mobility indicators. It consists of five major components: (1) dividing urban boundaries into a set of regular grids; (2) constructing multi-scale urban mobility networks; (3) proposing a set of network-based mobility measures, such as area connectivity, area popularity, neighborhood interaction, and mobility growth rate; (4) calculating urban indicators, including total footprint area of buildings, road net-network length, point of interest and gross domestic product; and (5) fitting scaling laws in both mobility and urban contexts and analyzing the derived scaling properties. This procedure is depicted in Figure 1 (Table 1).

3.2. Scaling laws in urban mobility

We began by converting travel-flow information into an urban mobility network. Specifically, we created a set of weighted directed networks representing distinct time periods by aggregating all individuals' flows. At a given timeslot t, the urban mobility network is defined as

$$G(t) = \{V, E(t), W(t)\} \tag{1}$$

where $V = distinct\left(\cup_{u=1}^{u=M} V(u)\right)$ represents all different urban areas (i.e. grid cells), in which M depends on the grid size, and $E(t) = \left(v_i, v_j\right)|\left(v_i, v_j\right) \in V$ represents all travel flows between pairs of areas. Edge weights $W(t)$ correlate to flow counts: for each individual flow on an edge $\left(v_i, v_j\right)$, the weight $W\left(v_i, v_j\right)$ is increased by one.

From June 2017 to June 2019, we chose one week of data from each month to aggregate into the monthly urban mobility network. Twenty-five networks were created to represent monthly urban mobility patterns. We then employed a set of urban mobility measures to investigate the properties of these urban mobility networks, including area connectivity, area popularity, area neighborhood interaction, and area mobility growth rate.

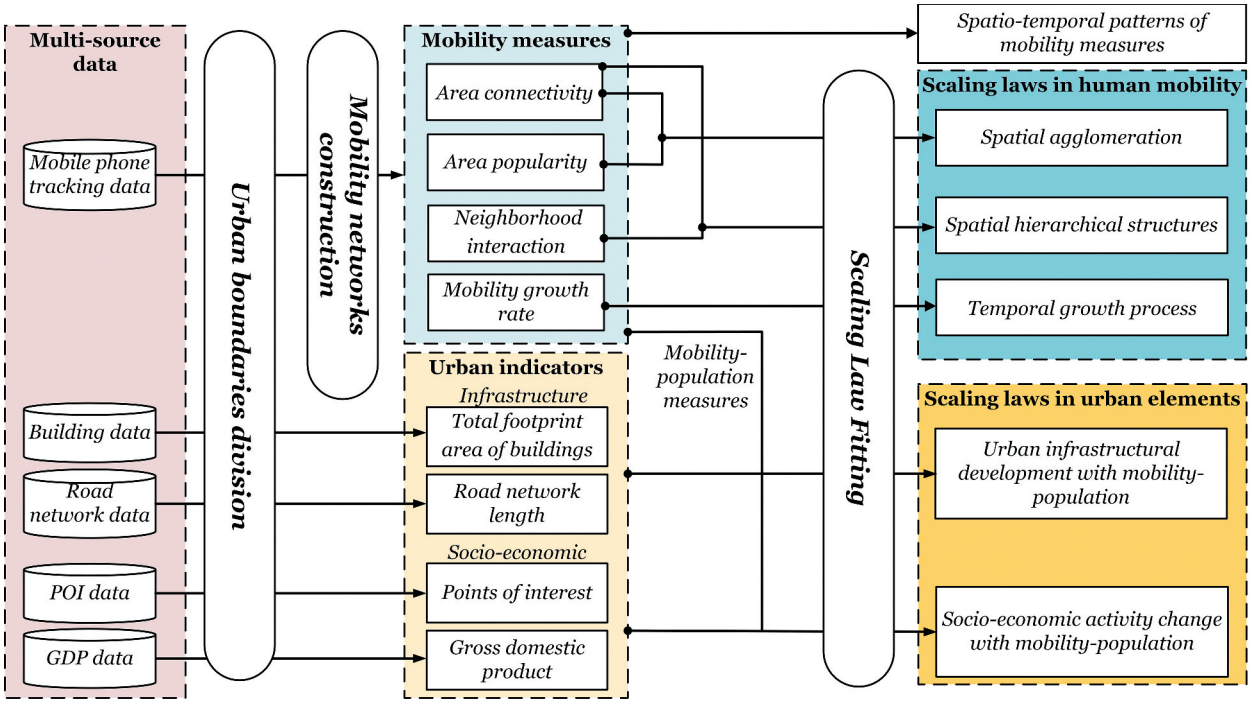

Figure 1. The workflow of the analytical framework.

Table 1. Urban indicators and corresponding data sources.

Characteristic	Indicators	Data sources
Infrastructure	Total footprint area of buildings	Building data
	Road network length	Road network data
Socio-economic activity	Points of interest	POI data
	Gross domestic product	GDP data
Population	Mobility-population measure	Mobile phone data
Mobility	Area connectivity	
	Area popularity	
	Neighborhood interaction	
	Mobility growth rate	

3.2.1. Urban mobility measures

3.2.1.1. Area connectivity. Area connectivity denotes the count of connected areas in a mobility network. Higher connectivity indicates that areas are more interlinked. The area connectivity k_i is calculated as the number of areas to which area i is connected within the network, denoted by

$$k_i = \sum\nolimits_{j \in V} N(v_i, v_j) \tag{2}$$

where $N(v_i, v_j) = 1$ when there is at least one connecting flow between area i and area j throughout the time period, and 0 when there is no flow between the two areas.

3.2.1.2. Area popularity. The popularity of an area is a metric used to highlight the geographical popularity of traveling flows. Higher popularity indicates that an area pulls more traveling flows from other areas and has the potential to be a hub area. This quantity is derived from the node strength in the urban mobility network, which is defined as the sum of the total travels $n_j^{(i)}$ of each area j, as illustrated in

$$s_i = \sum\nolimits_{j}^{N_i} n_j^{(i)} = \sum\nolimits_{j \in V} W(v_i, v_j) \tag{3}$$

where $W(v_i, v_j)$ equals the edge weight between area i and area j.

3.2.1.3. Neighborhood interaction. Neighborhood interaction captures the degree to which neighboring areas are associated with one another. A greater value suggests that inhabitants who visit a certain area also regularly visit its neighbors. This metric is represented in the urban mobility network by the clustering coefficient of each node i, which is defined as

$$c_i = \frac{1}{s_i(k_i - 1)} \sum\nolimits_{j,k} \frac{W(v_i, v_j) + W(v_j, v_k)}{2} a_{ij} a_{jk} a_{ki} \tag{4}$$

where a_{ij} are the elements of the adjacency matrix.

3.2.1.4. Mobility growth rate. The mobility growth rate reflects the expansion of an area's connectivity and popularity. The parameter $S_i(t)$ counts the cumulative number of travel flows directed to an area i up to

a particular period t. Similarly, $K_i(t)$ expresses the cumulative number of areas connected to area i up to the period t. The dynamics of $S(t)$ and $K(t)$ between t_0 and t_1 can be viewed as a growth process, with each area displaying a different growth rate; hence, growth rates for popularity and connectivity are designated as r_i^S and r_i^K, respectively, provided by

$$r_i^S = ln\frac{S_i(1)}{S_i(0)} \tag{5}$$

$$r_i^K = ln\frac{K_i(1)}{K_i(0)} \tag{6}$$

where for each area i, $S_i(1)$ and $S_i(0)$ are the cumulative volume of travels until t_1 and t_0, respectively, and $K_i(1)$ and $K_i(0)$ are likewise the cumulative tally of connected areas until t_1 and t_0.

3.2.2. Scaling laws between mobility measures

To investigate the spatio-temporal dynamics of mobility networks, we examined three scaling relations that characterize spatial agglomeration, spatial hierarchical structures, and the temporal growth process.

3.2.2.1. Spatial agglomeration. The first scaling law deals with urban mobility spatial agglomeration. In particular, this law designates the popularity distributions in urban areas with varying connectivity. The area popularity $s(k)$ is calculated as the averaged popularity of areas with connectivity k.

$$s(k) = \frac{1}{N(k)}\sum\nolimits_{i/k_i=k} s_i \tag{7}$$

where $N(k)$ is the number of areas with connectivity k.

We then examined whether the relation of $s(k)$ and k follows the law, determined by

$$s(k) \sim Ak^{\beta} \tag{8}$$

where β denotes the level of spatial agglomeration. $\beta > 1$ suggests a greater spatial agglomeration effect.

3.2.2.2. Spatial hierarchical structures. The second scaling law aids in the evaluation of neighborhood spatial structures and illustrates how spatial neighbor clusters are structured among nodes with varying connectivity, revealing patterns in spatial hierarchy. The neighborhood density $C(k)$ for areas with a certain connectivity k is determined by:

$$C(k) = \frac{1}{N(k)}\sum\nolimits_{i/k_i=k} C_i \tag{9}$$

where $N(k)$ is the number of areas having connectivity k.

This scaling relation provides a mechanism for detecting the presence of hierarchy in real-world networks. Such hierarchy may be well described using the scaling relationship demonstrated by the findings of Dorogovtsev, Goltsev, and Mendes (2002), given as

$$C(k) \propto k^{B\alpha} \tag{10}$$

A negative scaling relation ($\alpha < 0$) indicates that nodes with higher connectivity are likely to have fewer neighbors. A complete hierarchy is represented by $\alpha = -1$. There is no hierarchy in the network if $C(k)$ is independent of k.

3.2.2.3. Temporal growth process. The third scaling law investigates the time evolution of urban mobility. We take into account two variables: the conditional average growth rate $< r_S(S_0) >$ and the conditional standard deviation $\sigma_S(S_0)$. $< r_S(S_0) >$ measures the average increase in the number of trips performed between t_0 and t_1, given an initial travel volume of S_0. In other words, we simply evaluate the average growth rate of areas that have been visited S_0 times as of t_0. $\sigma_S(S_0)$ expresses the statistical dispersion or fluctuation of growth among included areas and is calculated by $\sigma_S(S_0) = \sqrt{< r_S(S_0)^2 > - < r_S(S_0) >^2}$. The expressions $< r_k(k_0) >$ and $\sigma_k(k_0)$ are defined in a similar way.

We then stole the argument from Gibrat's law, which is an economic law that states that the mean and standard deviation of a particular indicator's growth rate are both constant and independent of its initial value (Eeckhout 2004). In other words, both $\langle r_S(S_0) \rangle$ and $\sigma_S(S_0)$ are independent of S_0 (Rozenfeld et al. 2008; Rybski et al. 2009). $\langle r_k(k_0) \rangle$ and $\sigma_k(k_0)$ are are also unrelated to k_0, expressed as

$$\langle r_S(S_0) \rangle, \sigma_S(S_0), \langle r_k(k_0) \rangle, \sigma_k(k_0) = \text{const.} \tag{11}$$

This scaling law means that regardless of beginning conditions, each area has the same opportunity to grow at a certain rate. For example, an area with only 1000 starting visits has the same probability of doubling in a given period as an area with 100,000 visits.

3.3. Scaling laws in urban indicators

Intra-urban scaling laws are universal power-law representations of quantitative scaling relationships between urban indicators and gridded-level population, denoted as

$$Y_i \sim Y_0 P^{\beta} \tag{12}$$

where i signifies a grid cell within the city, Y_i denotes an urban indicator, P is the population size, β is the scaling exponent, and Y_0 is a normalization constant.

This study used total building footprint area and total road length to reflect urban infrastructure development, and POIs and GDP to indicate urban socioeconomic activity. Different urban indicators have

different scaling exponents (the value of β), as has been empirically proved (Gong and Xu 2021). For example, infrastructure-related variables (e.g. total length of electrical cables, total road surface) typically have an exponent $\beta < 1$, indicating that the variable will scale sub-linearly with population size due to economies of scale, resulting in enhanced efficiency. Meanwhile, due to endogenous social interactions, social interaction-related indicators (e.g. crime rate) normally scale super-linearly ($\beta > 1$), but individual-related indicators (e.g. income, household energy consumption) typically scale linearly ($\beta \approx 1$) (Jiao et al. 2021).

In order to discover a more accurate measure of urban population distribution, we consider the mobility of the gridded population as alternative to the basic registered population counts usually provided in official city statistics. Specifically, we employ a mobility population measure for areas, which is a more appropriate proxy for population distribution. In this study, this measure is estimated from a massive mobile phone dataset; for a complete explanation of the data, see the "Study area and data" section.

3.4. Function fitting for the scaling laws

Scaling laws represent a nonlinear, quantitative relationship between two measures. The universal version of the power-law may be used to describe the relationship between measures Y and X within area i at a single time point t:

$$Y_i(t) \sim X_i(t)^{\beta} \tag{13}$$

where β corresponds to the scaling exponent.

To calculate the scaling exponent, we take the logarithms of both axes and derive the linear connection between $\log Y_i(t)$ and $\log X_i(t)$. The logarithms are then fitted using linear Ordinary Least-Squares (OLS) regression, with the slope representing the scaling exponent:

$$\log Y_i(t) = \beta \log X_i(t) + \log Y_0 + \sigma_i \tag{14}$$

where Y_0 and σ_i are the constant and the fitting residual, respectively, and β is the estimated scaling exponent.

4. Results and discussion

4.1. Study area and data

Shenzhen was chosen as the study area; this metropolis is located in southern China and has an area of approximately 2000 km^2. As of 2019, it contains nine sub-administrative districts and one new district. Figure 2(a) depicts a spatial map of Shenzhen. Shenzhen intensified its urbanization process after reform and opening up forty years ago, and it has since developed into a well-known, world-class megacity. According to the Seventh National Census ("Communiqué of the Seventh National Census of Shenzhen" 2021), Shenzhen's residential population was 17.56 million as of the end of 2020, up 7.13 million (68.46%) in ten years. As a result, the population density reached 8793 people/km^2, the highest in China. This massive influx of people contrasts sharply with the city's limited urban capacity, highlighting the urgent necessity to assess urban system growth in relation to many urban characteristics and to utilize the findings to assist future urban policy.

To calculate typical urban and mobility measurements, we integrate information from a number of data sources. Namely, we employ five large datasets: building footprints, road networks, POIs, estimated GDP, and mobile phone location tracking. Their details are described below.

4.1.1. Building data

The building data was collected from a digital map of China. A total of 699,406 spatially arranged building-level blocks were included. Building attributes include building footprint and number of floors. Figure 2(b) depicts the geographical layout of these buildings. The data from buildings were utilized to demonstrate urban infrastructure development.

4.1.2. Road network data

Road networks with a total of 13,834 road segments were downloaded from OpenStreetMap (OSM) (http://www.openstreetmap.org/) in June 2020. Figure 2(c) displays the geographical dispersion of these networks. The total length of road networks in different areas is another infrastructural-related indicator used to measure spatial accessibility.

4.1.3. POI data

We gathered POI data from GaoDe, China's largest online map service provider. The raw data has 16 kinds of venues, including stores, restaurants, and daily life services. There are about 681,241 POIs. Figure 2(d) exhibits the spatial distribution of these POIs. The POI distribution is used to illustrate socio-economic activity.

4.1.4. GDP data

Kilometer-gridded GDP data was derived from a publicly available product (Xu 2017) that was obtained by a space allocation method that comprehensively considers land-use types, night light brightness, residential density, and other factors closely related to human economic activities based on the official statistical communique for the year 2019. The spatial distribution of estimated GDP is depicted in

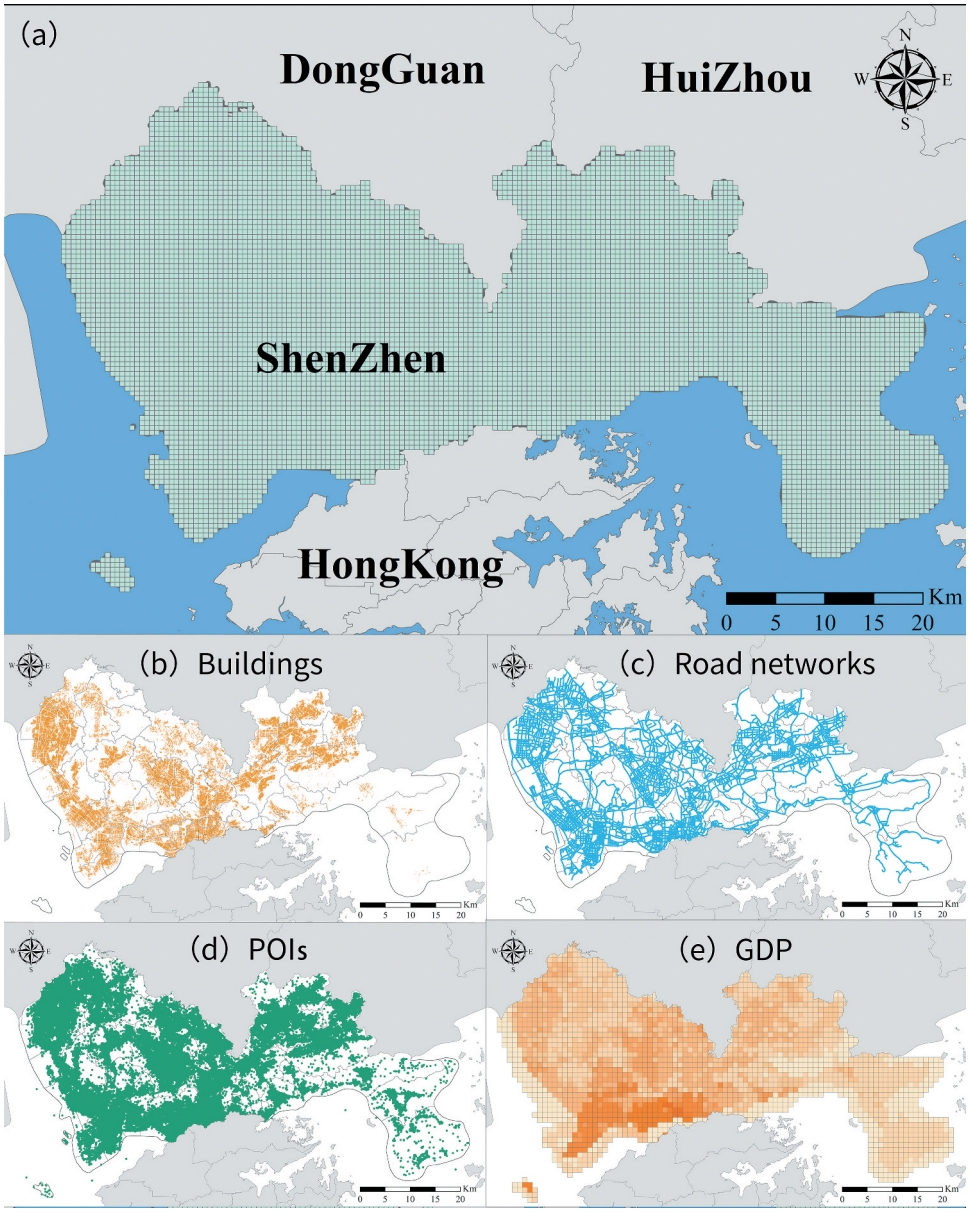

Figure 2. The geographical layout of (a) 500 m regular grids, (b) buildings, (c) road networks, (d) POIs, and (e) GDP in the city of Shenzhen.

Figure 2(e). The GDP count is also used to reflect urban socioeconomic activity.

4.1.5. Mobile phone data

Granular mobile phone tracking data was gathered from a leading Chinese communication operator. From 2017 to 2019, the dataset tracked long-term phone users' stay activities and movements between signaling towers. However, due to a rigorous privacy protection policy, we were only able to obtain spatially aggregated data and not individual data. As a result, the gathered data did not expose any personal information, and the operator transformed the positions of stay activities to grid cells. The data reveals information in two forms: data aggregated at the grid cell level, such as total users or tallied home locations within each cell, and daily travel flows between any given pair of cells, with each travel-flow record consisting of origin-cell id, destination-cell id, and population count comprising the flow between. Using this aggregated data, we developed a mobility-population measure as an alternative to static population and calculated several indicators of urban mobility across time to capture population and flow patterns.

In general, the large, fine-grained datasets employed in this work allow for more precise exploration of intra-urban scaling laws and the development of greater insights. The framework for measuring scaling laws in this study context is discussed in the next section.

4.2. Spatio-temporal patterns of mobility indicators

Figure 3 depicts the month-by-month distributions of four urban mobility measures collected from urban

mobility networks across Shenzhen from June 2017 to June 2019. Month-averaged area connectivity, popularity, and neighborhood interaction all showed similar tendencies, namely an overall steady increase from June 2017 to June 2019, with the exception of a dip around February each year. This variation was closely tied to the Chinese Spring Festival, during which many people leave to visit their hometowns, resulting in a significant fall in the mobility population in Shenzhen. The average growth rate fell roughly 52% from 2.3 in July 2017 to 1.2 in February 2018, after which it remained low, demonstrating that urban trips maintained a consistent low growth.

Figure 4 illustrates the spatial distributions of the four mobility measures in July 2019; the results for other months were similar. These mobility indicators differ in their spatial distribution. With regard to area connectivity, highly connected areas are reasonably well distributed among the urban central districts, including Futian, Nanshan, and Luohu (Figure 4(a)); conversely, sub-urban areas, particularly those in North and Northeast Shenzhen, exhibited low levels of connectivity. Regarding area popularity, a cluster of highly popular areas concentrated in central urban districts, and there is significant overlap between areas with higher connectivity and those with higher popularity (Figure 4(b)). The populated distribution in the urban center, on the other hand, is more spatially centralized and aggregated than the connectivity distribution, indicating a spatial agglomeration effect. Surprisingly, the suburbs and outskirts show significant levels of neighbor interaction, which contrasts with the spatial distributions of area connectivity and popularity (Figure 4(c)) and suggests a hierarchical structure of urban mobility networks. Finally, the travel growth rate showed a completely opposite pattern, with slower growth rates in more popular areas. Higher growth rates were observed in several

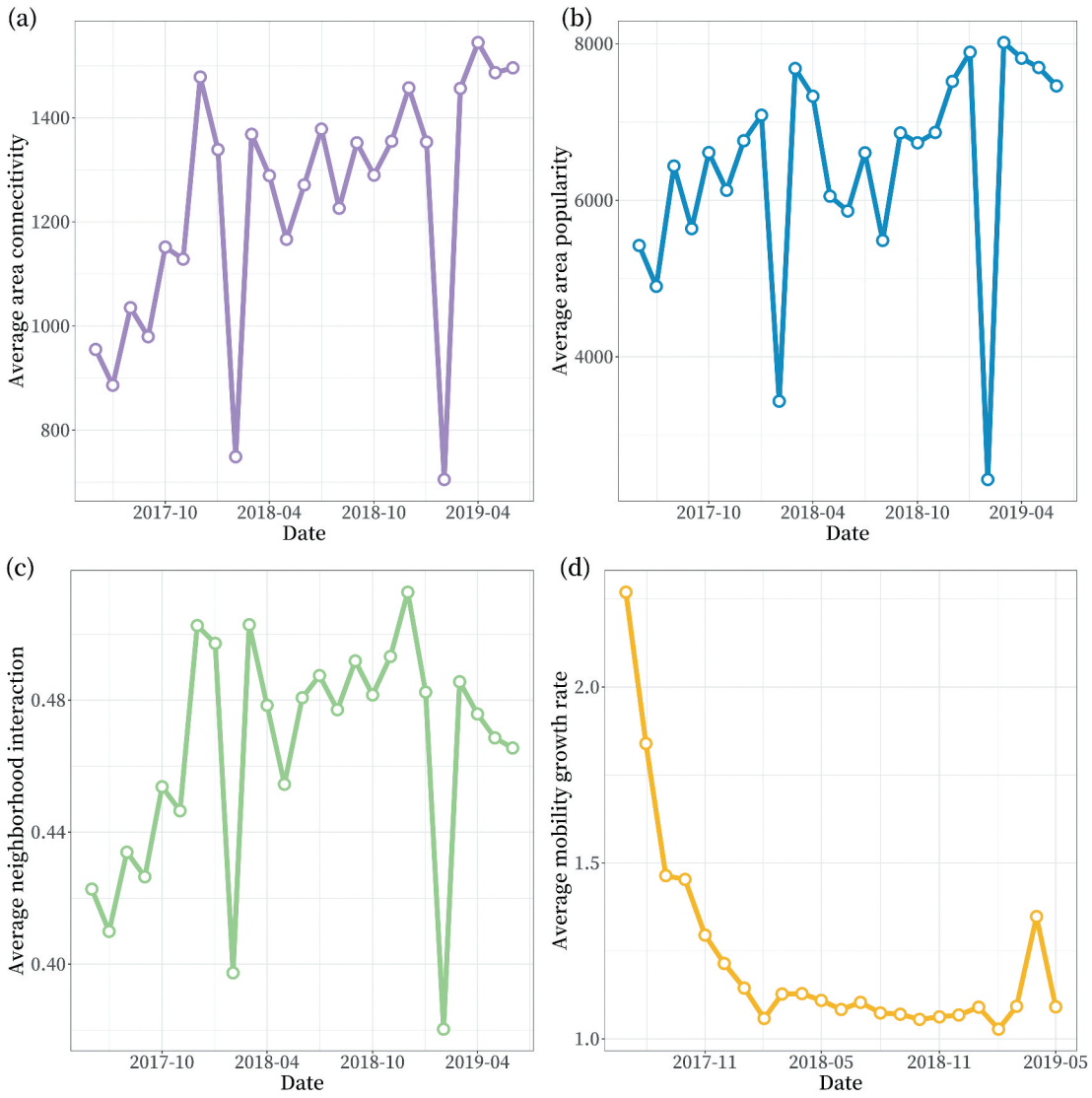

Figure 3. Monthly variation in four urban mobility measures from June 2017 to June 2019: (a) area connectivity; (b) area popularity; (c) neighborhood interaction; and (d) mobility growth rate. "201710" denotes October 2017, and other month periods are similarly denoted.

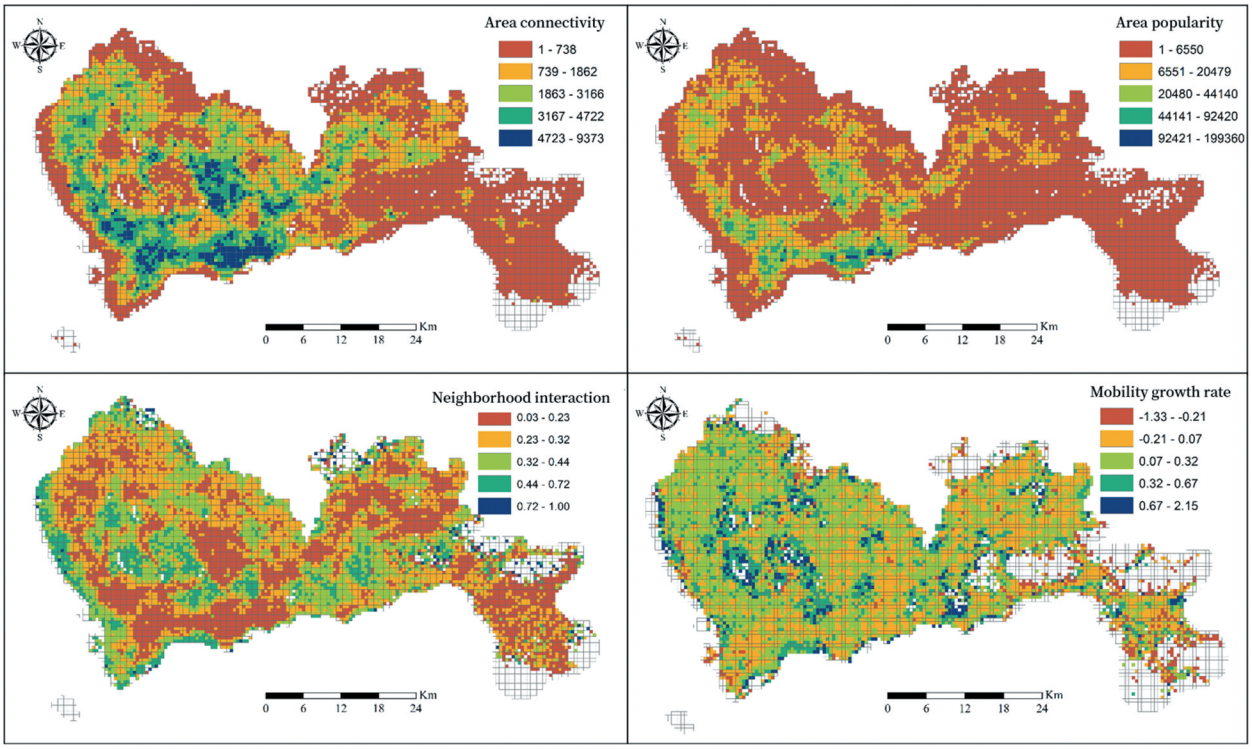

Figure 4. Spatial distributions of four urban mobility measures for July 2019: (a) area connectivity; (b) area popularity; (c) neighborhood interaction; and (d) mobility growth rate. Blue indicates higher values and yellow smaller values. No color means no data.

promising development areas, notably Bao'an, Longhua, and Yantian (Figure 4(d)).

These results imply that the temporal and spatial distributions of urban mobility measures inside a megacity reveal unseen similarities and differences, and that a scaling-law examination of their relationships is required to better understand them.

4.3. Scaling laws in mobility measures

The scaling relations of measures defining three components of urban mobility are examined here: spatial agglomeration, spatial hierarchical structures, and the temporal growth process. We examined these three scaling laws through three very simple and easy-to-understand formulas that investigated the relationships between two explainable urban mobility measures.

The first scaling law concerns spatial agglomeration. Figure 5(a) depicts the relationship between area popularity and area connectivity, which when plotted in double logarithmic coordinates resembles a straight line, as predicted by the law of $s(k) \sim Ak^{\beta}$. The exponents are calculated using OLS analysis with bootstrapped 95% confidence. Interestingly, the β values are greater than 1 for all three years of the study period, indicating a robust super-linear scaling of area popularity with connectivity. In other words, the $\beta > 1$ regime supports a spatial agglomeration effect in urban travel, demonstrating that more highly connected areas attract a disproportionately larger number of travel flows. This finding shows that increasing urban connectivity will expedite population flows.

From 2017 to 2019, the scaling exponent β continuously grew, indicating that Shenzhen's spatial agglomeration is increasingly strengthening. Variation in scaling exponents among ten Shenzhen districts is shown in Figure 5(d), with the coefficient difference between 2017 and 2019 arranged on the horizontal axis in ascending order. During that three-year period, Longgang District had the least coefficient difference, and Pingshan District the greatest. In general, areas with smaller coefficients in 2017 expanded more quickly in 2018 and 2019. These findings suggest that Shenzhen's spatial agglomeration effect has featured significant spatial variability in the last two years. A lower agglomeration effect might potentially draw disproportionate flows, progressively increasing the aggregation effect over time.

The second scaling law has to do with spatial hierarchical systems. Figure 6 depicts the empirical behavior of a spatial area's neighborhood density and connectivity over three years. According to the law of $C(k) \propto k^{B\alpha}$, the fitted lines represent decreasing power-law scaling. These decreasing relationships imply that metropolitan regions with denser communities do not have higher connectivity; rather, the opposite is true. For the three-year period examined,

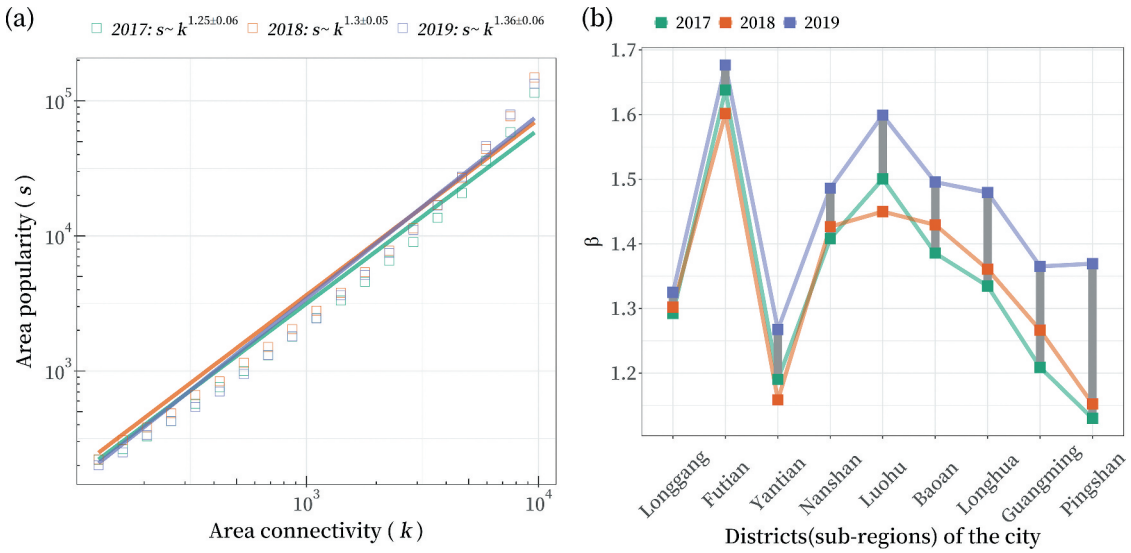

Figure 5. The relationship of area connectivity and popularity in Shenzhen for the years 2017, 2018, and 2019. (a) Robust super-linear scaling is observed for all three years. Colored lines show the respective fit of β for 2017 (green: $\beta = 1.25 \pm 0.06$ [95% confidence interval], $R^2 = 0.94$), 2018 (orange: $\beta = 1.30 \pm 0.05$ [95% confidence interval], $R^2 = 0.91$), and 2019 (purple: $\beta = 1.36 \pm 0.06$ [95% confidence interval], $R^2 = 0.92$). (b) Variation of the scaling exponent β in ten districts of Shenzhen.

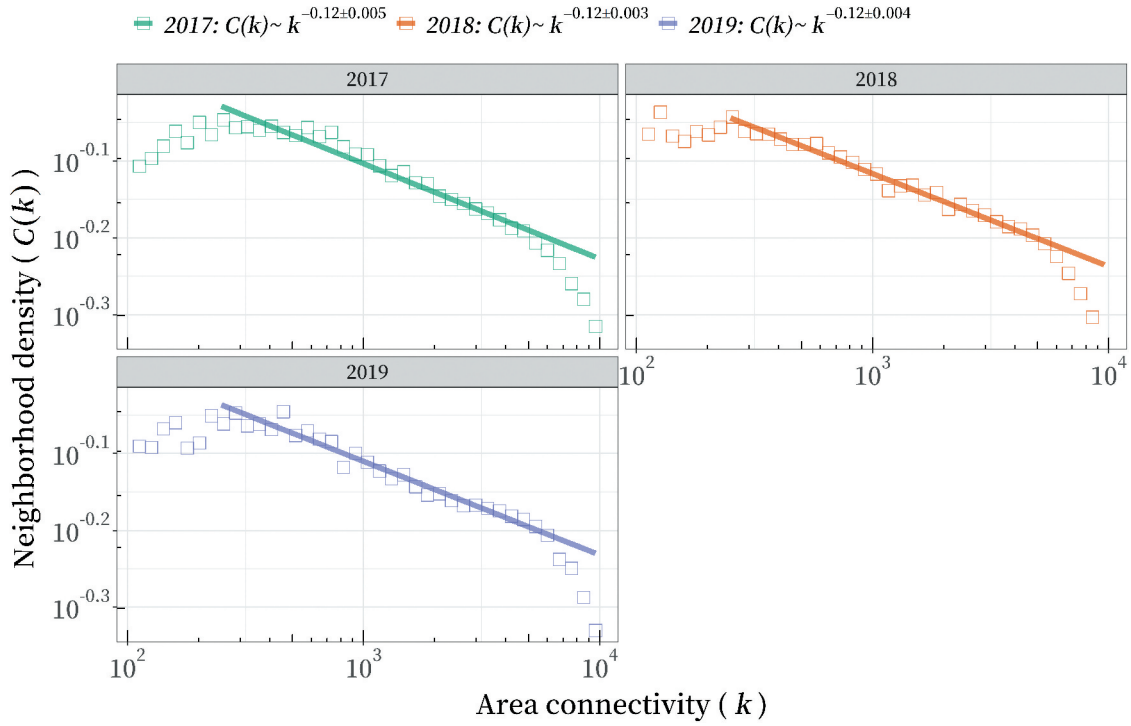

Figure 6. Intra-urban mobility scaling laws between neighborhood density and area connectivity from 2017, 2018, and 2019. The colored lines represent the decreasing power-law fits for 2017 (green: $\alpha = -0.12 \pm 0.005$ [95% confidence interval], $R^2 = 0.94$), 2018 (orange: $\alpha = -0.12 \pm 0.003$ [95% confidence interval], $R^2 = 0.92$), and 2019 (purple: $\alpha = -0.12 \pm 0.004$ [95% confidence interval], $R^2 = 0.94$).

the fitted scaling exponents of α are smaller than zero, indicating that hierarchy is present.

According to Dorogovtsev, Goltsev, and Mendes (2002), networks having scaling relations of the type $C(k) \propto k^{B\alpha}$ are regarded as hierarchical, with a scaling exponent of $\alpha = -1$ signifying a perfect hierarchy. A hierarchical network structure implies that sparsely connected areas tend to be part of highly clustered areas, with only a few hubs providing links between the various highly clustered neighborhoods; that is, a few local hubs attract substantial travel flows and form hierarchically poly-centric groups within the

city. Each group is internally heterogeneous (Ravasz and Barabási 2003). We noticed empirically that Shenzhen followed this relationship with $\alpha = -0.12$ during the three-year study period. This discovery indicates that the metropolis has a developing hierarchical structure, which is consistent with its status as the world's fastest-growing city.

The third scaling law examines the temporal growth dynamics of urban mobility. Figure 7 depicts two typical instances of travel volume growth trends for two areas. Figure 7(a,b) illustrate the monthly travel volumes for those areas, which are represented by blue and yellow pillars. It is clear that the two areas have distinct patterns. The monthly cumulative number of travels for each area is shown in Figure 7(c). Clearly, the blue area has faster growth at both the beginning and end of the study period and much less in the middle, whereas the yellow area displays only tiny temporal changes. The travels of the two areas are depicted in Figure 7(d), together with the periods in which those travels occurred.

The growth rates of area travel volumes were computed by dividing r by the time period $t_1 - t_0$. The conditional average growth rate $\langle r_S(S_0)\rangle$ versus the initial travel volume S_0 is depicted in Figure 8(a). We discovered that $\langle r_S(S_0)\rangle$ decreases as a power law of the following form:

$$\langle r_S(S_0)\rangle \sim S_0^{-\alpha} \tag{15}$$

We also performed an OLS regression analysis with bootstrapped 95% confidence and found the mean growth exponent to be $\alpha_S = -0.3 \pm 0.004$. Due to the small sample size, area-specific values differed somewhat for large S_0.

Figure 8(b) shows the dependence of the standard deviation in growth $\sigma_S(S_0)$ on S_0. On average, the growth rate of more populated areas fluctuates less than that of less populated areas, which contradicts Gibrat's law. As a result, the power law, where β_S is the standard deviation exponent and $\beta_S = -0.56 \pm 0.01$, better approximates this finding. Because this measure is regulated by a power law, fluctuations in growth are

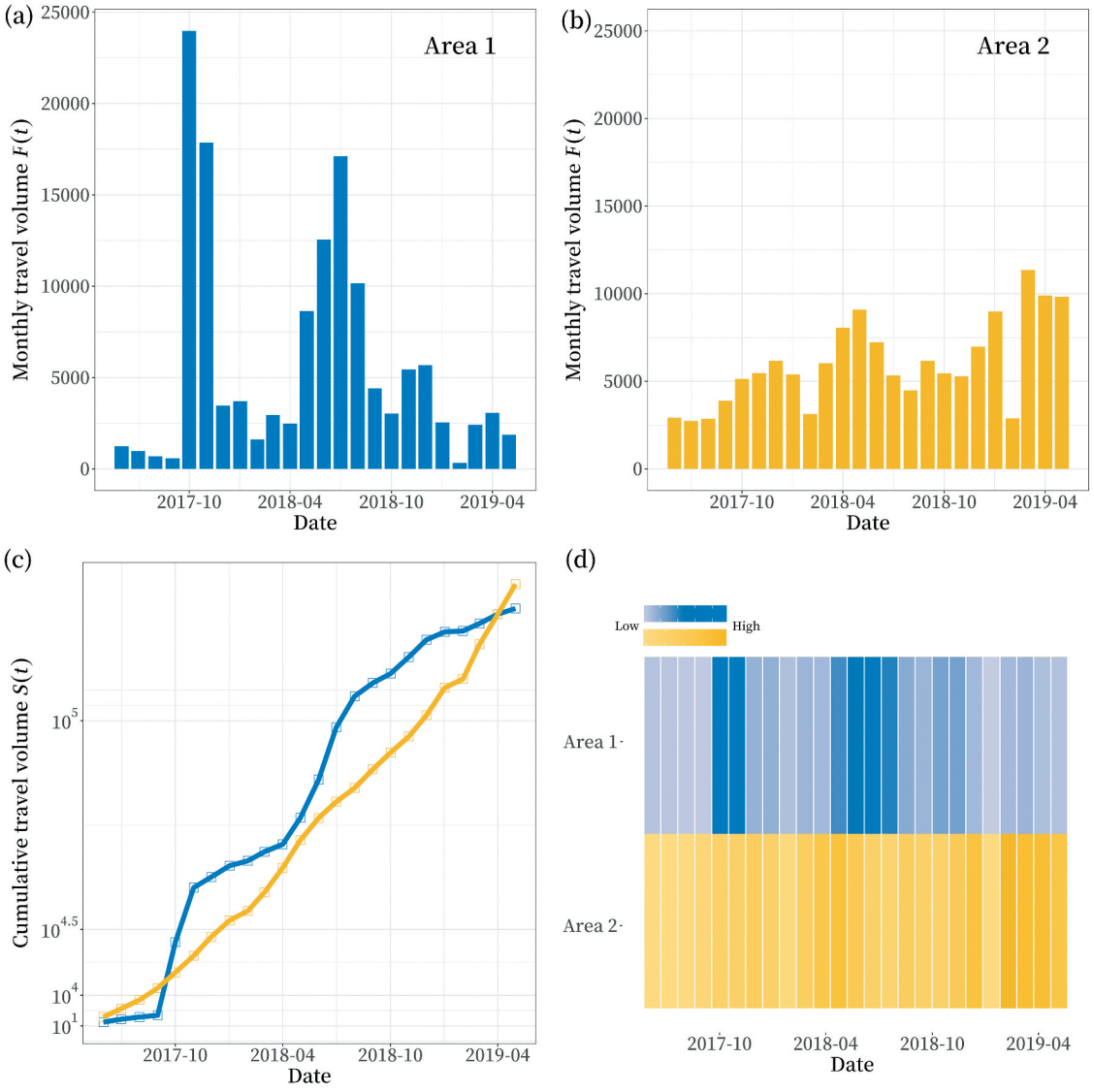

Figure 7. Two typical volume growth patterns for area-level travel. (a–b) Monthly travel volumes, (c) monthly cumulative travels, and (d) monthly total travels for two typical areas, shown in blue and yellow.

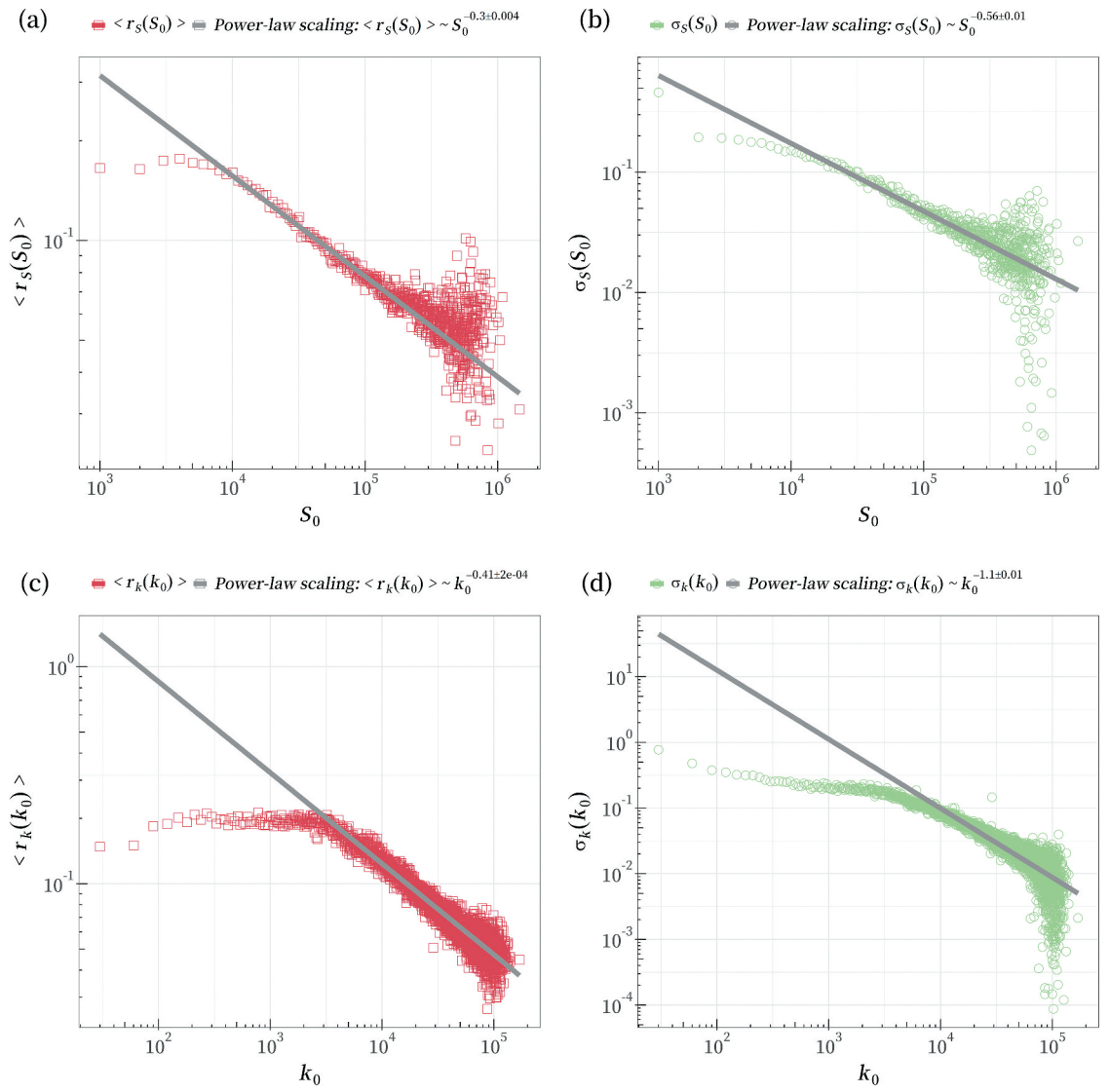

Figure 8. Intra-urban mobility scaling laws for temporal growth of traveling activities in Shenzhen from 2017 to 2019. (a) the average growth rate conditional on S_0,$\langle r_S(S_0)\rangle$, decays with exponent $\alpha_S = -0.3 \pm 0.004$. (b) the standard deviation decays with exponent $\beta_S = -0.56 \pm 0.01$. (c) the growth rate of area connectivity conditional on k_0 decays with exponent $\alpha_K = 0.41 \pm 0.002$. (d) the standard deviation decays with exponent $\beta_K = 1.1 \pm 0.01$.

statistically self-similar across scales for initial traveling volumes ranging from 10^4 to 10^6.

$$\sigma_S(S_0) \sim S_0^{-\beta} \tag{16}$$

Figure 8(c,d) depict results pertaining to the conditional growth rate of area connectivity. OLS regression analysis on the average growth rate $r_k(k_0)$ revealed a tendency to power-law decrease with exponent $\alpha_K = 0.41 \pm 0.002$; meanwhile, the standard deviation $\sigma_k(k_0)$ exhibited large fluctuations as a function of K_0, especially for less-connected areas, and also shows a power-law decrease with K_0 with $\beta_K = 1.1 \pm 0.01$. We may argue that the standard deviation of the growth rate also deviates from Gibrat's law.

$$\langle r_k(k_0)\rangle \sim k_0^{-\beta} \tag{17}$$

$$\sigma_k(k_0) \sim k_0^{-\beta} \tag{18}$$

Based on the above results, we find that both quantities $r_S(S_0)$ and $r_k(k_0)$ do not follow Gibrat's law and show a decreasing trend in power-law form. Moreover, the growth process exhibits a divergent posture: areas with lower popularity grow faster, meaning that sparsely populated areas gradually catch up with the more populous in terms of travel activities.

4.4. Scaling laws in urban indicators

The fitting results for the mobility population measure and infrastructural-related indicators are depicted in Figure 9. We represented infrastructure in terms of the total footprint area of buildings and total length of road networks. We observed building footprint area to have a sub-linear scaling regime in relation to population, as can be seen in Figure 9(a). Overall, the rate of increase in building footprint area is about half

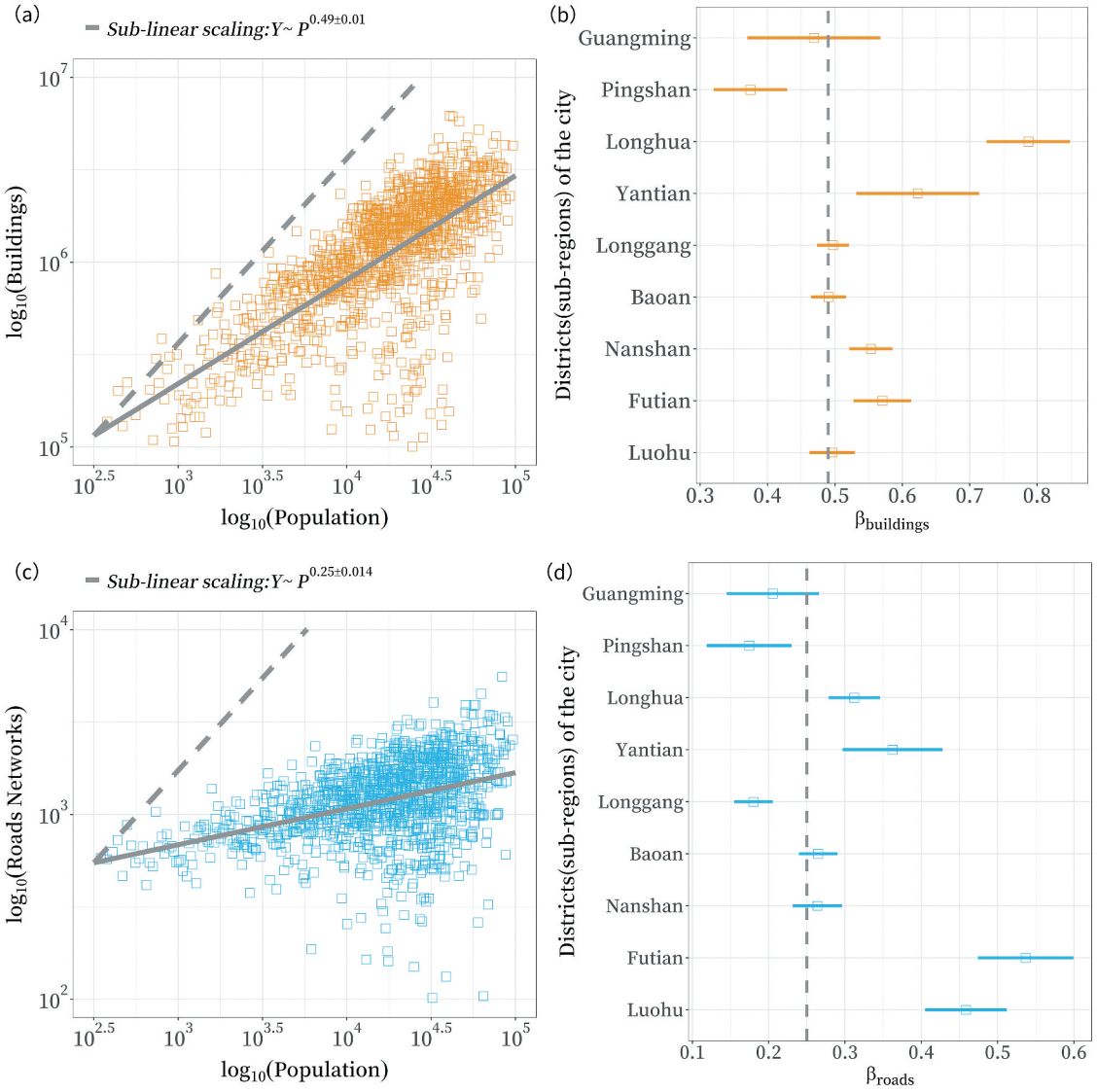

Figure 9. Intra-urban scaling of Shenzhen infrastructure. (a–b) Scatter plots and fitting results for building volume: overall (a) and cross-district (b) sub-linear scaling between building footprint area and population. (c–d) Scatter plots and fitting results for road length: overall (c) and cross-district (d) sub-linear scaling between total length of road networks and population. The solid line denotes the fitted scaling law, and the dashed line linear scaling.

that of the population because $\beta_{buildings}$ is around 0.5; that is, doubling the population within the grid requires only a 0.5 times increase in building capacity, reflecting an economy of scale effect owing to building verticality. Notably, the sub-linear scaling of infrastructure-related indicators with urban population varies among different types of infrastructure. Scaling analysis of road networks revealed that β_{roads} is also less than one, as illustrated in Figure 9(c), indicating a sub-linear scaling relationship with population. However, the difference between $\beta_{buildings}$ and β_{roads} means that when doubling the population in a grid region, 49% increase in buildings is needed but only 25% increase in road networks. This conclusion is similar to the findings of previous research done at the inter-urban level, demonstrating that a large economy of scale effect exists for infrastructure-related indicators at both inter-urban and intra-urban levels.

Different districts also experienced different levels of super-linear scaling relationship. We conducted scaling analysis for ten districts (sub-regions) in the study area for both of the abovementioned infrastructure-related indicators and found the exponents to be less than 1 across all districts, as shown in Figure 9(b,d). This finding indicates the robustness of this scaling law. The maximum value obtained for $\beta_{buildings}$ is over 0.7 (Longhua District) and the minimum is less than 0.37 (Pingshan District). A larger $\beta_{buildings}$ indicates that the demand for infrastructure is higher relative to population increase. Meanwhile, the lowest exponent values for road networks was likewise obtained in Pingshan District (around 0.17) while the highest value was observed for Futian District (around 0.54). With

Pingshan District having the lowest values for both $\beta_{buildings}$ and β_{roads}, it can be concluded that this area has a low level of infrastructure utilization. The observed differences in sub-linear scaling of infrastructure-related variables with respect to urban population further imply that different areas within cities show different levels of infrastructural development.

We then considered POI counts and GDP as proxy variables representing socioeconomic activity. These two indicators are closely related to social interaction, which has been revealed to have a super-linear scaling regime at the inter-urban level. However, Figure 10 illustrates that at the intra-urban scale, both variables exhibit sub-linear or nearly linear scaling. β_{POI} is 0.98, which is almost equal to 1, indicating a linear scaling relationship of POIs and population (Figure 10(a)). This linear scaling regime describes the refined facilities in a community as being proportionate to the intra-urban population size. Interestingly, GDP has a sub-linear scaling regime with population (Figure 10(c)), with $\beta_{GDP} = 0.44 \pm 0.01$. This is inconsistent with the previously-reported theoretical cross-city value of the scaling exponent between GDP and population (Gong and Xu 2021). We speculate that this is mainly attributable to the city having a strong economy in aggregate but unbalanced GDP output among different regions.

The results of the scaling analysis of socioeconomic activity for ten districts are shown in Figure 10(b,d). In general, most districts have POI scaling exponents that are larger than one, showing a super-linear scaling relationship. The largest exponents were observed for Luohu District, Futian District, Baoan District, and Nanshan District, which are the most densely populated and most well-equipped areas in Shenzhen, indicating that increases of population in these areas necessitate

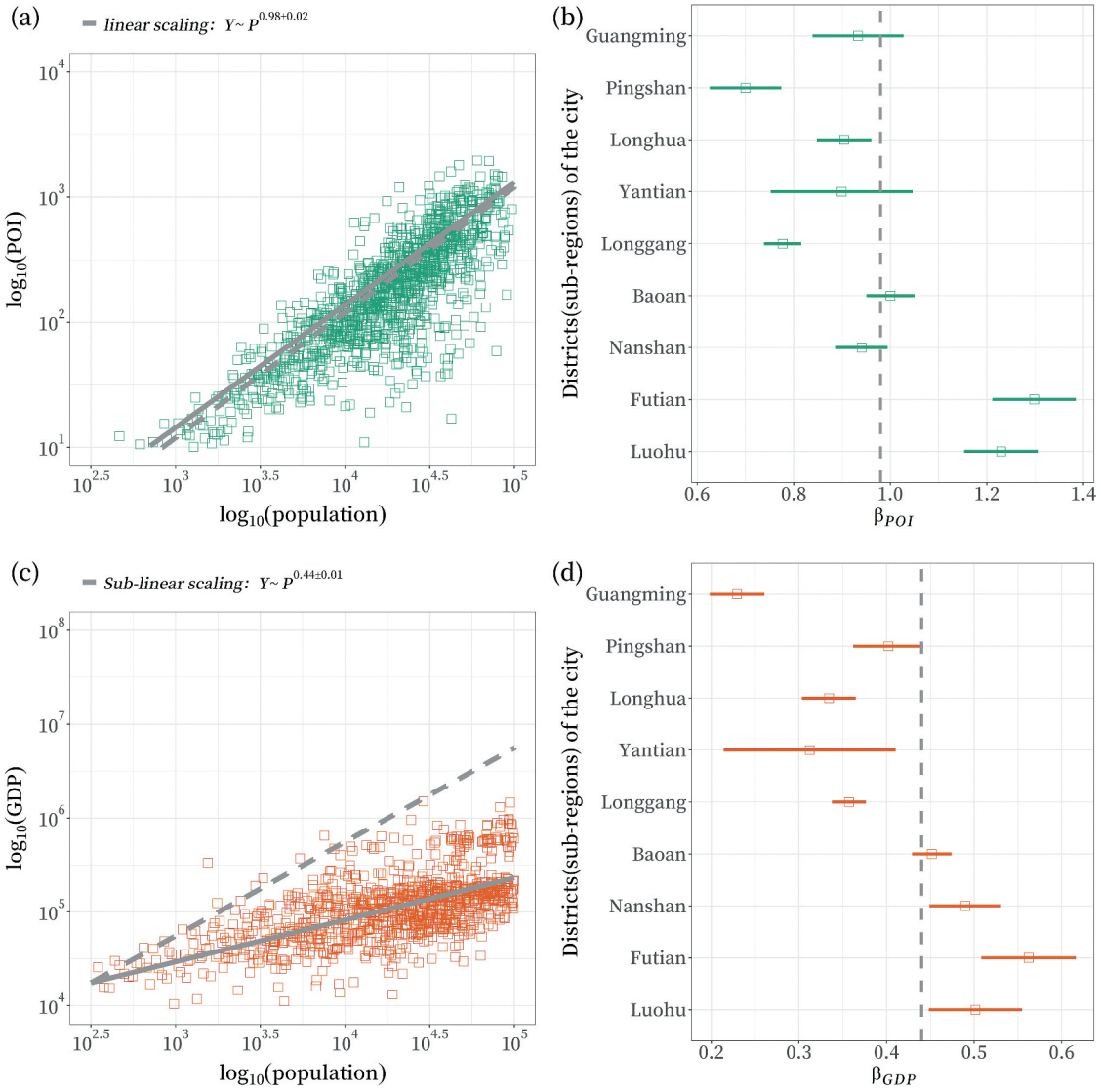

Figure 10. Intra-urban scaling of socioeconomic interaction measures for Shenzhen. (a–b) Scatter plots and fitting results for number of POIs: overall (a) and cross-district (b) variation of scaling between number of POIs and population. (c–d) Scatter plots and fitting results for GDP: overall (a) and cross-districts (b) variation of sub-linear scaling between number of POIs and population. The solid line denotes fitted scaling, and the dashed line linear scaling.

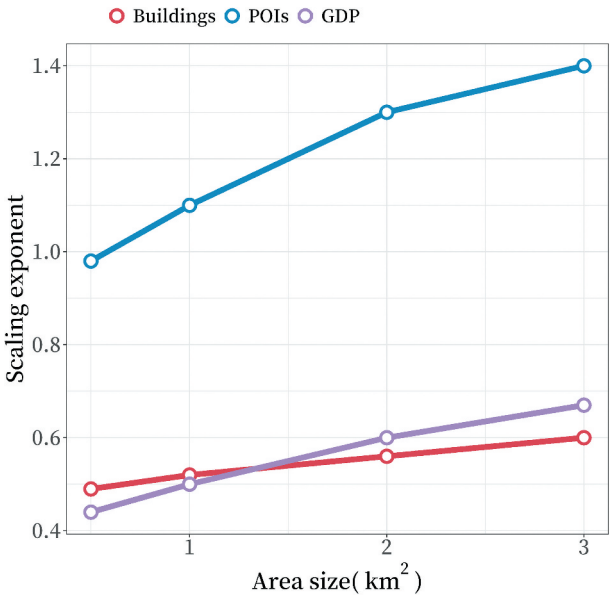

Figure 11. Scaling exponent value by grid size.

more growth in facilities. All ten sub-regions also exhibited GDP scaling exponents that were less than one, indicating a robust sub-linear scaling relationship with population. Again, the largest exponents were associated with Futian District, Luohu District, Nanshan District, and Baoan District, indicating that population growth in these four districts makes a greater contribution to GDP increase.

Given that urban indicators have complex spatial distributions, statistical analysis requires that a proper spatial unit be employed; that is, the choice of unit may impact observed robustness. A situation in which analysis results are impacted by the spatial aggregation unit (Longley 2017) is referred to as a Modifiable Areal Unit Problem (MAUP). To correct this potential MAUP, we also performed a robustness check by varying grid size (Figure 11). The results revealed that all fitting scaling laws are scale-insensitive and stable.

5. Conclusions

Scaling laws that characterize urban mobility and urban elements have the potential to greatly advance our understanding of urban development; in addition, the dynamic adherence of human mobility networks to scaling laws may also explain trends observed in other fields. Current scaling law frameworks usually investigate macroscopic scaling across cities, modeling each city as a whole and ignoring heterogeneous intra-urban patterns. Moreover, previous studies mostly focused on explaining scaling laws for static urban features, resulting in a lack of a comprehensive grasp of scaling laws pertaining to urban indicators and mobility measures. In this study, we devised a framework for measuring intra-urban scaling laws in terms of both urban indicators and mobility measures at the meter level.

Empirical application of this framework to the city of Shenzhen, China yielded several findings. Analyzing the properties of urban mobility scaling laws indicated scaling laws to have effects on spatial agglomeration, spatial hierarchical structure, and temporal growth. Area connectivity in various areas of the city is proposed as a potential component in the diversity of area popularity, and locally highly-connected areas may induce a scale-up effect in urban mobility and generate excessive attraction. The spatial hierarchical patterns imply that this rapidly growing metropolis is evolving into a hierarchically polycentric structure. The temporal dynamics of urban mobility indicate a diverging trend – areas with low popularity increase more quickly, allowing sparsely inhabited areas to progressively catch up with more populous areas, indicating an urban self-organization effect. The results also demonstrate a strong sub-linear association between infrastructure volume and population, as well as a sub-linear relationship of socioeconomic activity with population, suggesting that scaling rules exist in intra-urban systems but differ from those that operate at the inter-urban level.

The proposed approach and its results are complementary to existing urban research yet have a different but typical urban setting, and so stand to enhance urban decision-making. The quantitative scaling laws permit the use of quantitative descriptions to comprehend urban phenomena within cities and so aid in the systematic management of cities, better anticipation of scenarios by policymakers, and fresh discoveries pertaining to intra-urban growth. For example, it might be unreasonable to evaluate an area's development efficiency in terms of total GDP or total infrastructure; instead, dynamic per capita demand should be considered because at the intra-urban scale, per capita GDP drops as the dynamic population grows, demonstrating economies of scale rather than incremental effects at the urban system scale. In addition, the findings suggest prospective urban planning initiatives. The observed super-scaling of area popularity, hierarchically polycentric structure, and self-organization effects of urban mobility all support the conclusion that intra-urban systems may also achieve self-similarity in the allocation of urban resources such as infrastructure and amenities. As a result, future urban development strategies should pay more thought to resource allocation in order to increase element efficiency, taking into account the scaling form of intra-urban mobility.

This study has several limitations. Firstly, we acknowledge that multi-sourced urban data might be biased. Because high-quality data sets are usually unavailable, proxy data is commonly used to represent urban features and human mobility. Relying on these data may not affect the overall patterns observed for urban structure and dynamics, but may impact the

robustness and reliability of the results. The growing availability of appropriate data sources, such as official population and GDP data, may offer a better picture. Secondly, the mechanism behind these findings is not fully examined in this study; we provide a micro view on the interaction between urban features and human mobility, and different cities may have different development logistics. This article used the single city of Shenzhen as the study area due to the ease of data collection; given the availability of data from cities globally, of course, our research should be expanded to other metropolitan regions to complement and explain these findings, and to assess the generality of intra-urban scaling laws. Finally, our developed measures are rather simple and might be improved to incorporate more comprehensive measures and additional urban characteristics in order to capture more complex urban aspects.

Disclosure statement

No potential conflict of interest was reported by the authors.

Funding

This research was supported by the National Natural Science Foundation of China [grant numbers 42001393, 42071360, 71961137003 and 42101472], the Basic Research Program of Shenzhen Science and Technology Innovation Committee [grant number JCYJ20220530152817039], the Natural Science Foundation of Guangdong Province [grant number 2019A1515011049] and the Key Laboratory of National Geographic Census and Monitoring, MNR [grant number 2020NGCMZD02].

Notes on contributors

Jinzhou Cao is currently an Assistant Professor at Shenzhen Technology University (SZTU) in the College of Big Data and Internet. He earned his PhD in Geographic Information Science (GIS) from the State Key Laboratory of Information Engineering in Surveying, Mapping and Remote Sensing (LIESMARS), Wuhan University. His research interest and expertise areas include Urban Big Data Mining, Geo-AI, and Urban Analytics on the Interaction between Human Mobility and Urban Environments.

Wei Tu is currently an Associate Professor with the Department of Urban Informatics, Shenzhen University. He is also a Visiting Scholar with the Senseable City Laboratory, Massachusetts Institute of Technology. His research interests include urban informatics, smart mobility, and urban spatial intelligence.

Rui Cao is currently a Research Assistant Professor at the Department of Land Surveying and Geo-Informatics (LSGI) and the Smart Cities Research Institute (SCRI), The Hong Kong Polytechnic University. His research interests lie in Geospatial Artificial Intelligence (Geo-AI) and Urban Informatics.

Qili Gao is a Research Fellow at the Centre of Advanced Spatial Analysis (CASA), University College London (UCL). She received her PhD in GIS from Wuhan University, China. Her research interests include spatial-temporal data mining, urban informatics, and human mobility analytics toward urban sustainability and human-centred urban planning.

Guanzhou Chen is currently an Assistant Researcher (post-doc researcher) with the State Key Laboratory of Surveying, Mapping and Remote Sensing, Wuhan University. His research interests include remote sensing, computer vision, and spatial intelligence.

Qingquan Li is currently a Professor with Shenzhen University and Wuhan University. His research areas include 3-D and dynamic data modeling in GIS, location-based service, surveying engineering, integration of GIS, global positioning system and remote sensing, intelligent transportation system, and road surface checking.

ORCID

Jinzhou Cao http://orcid.org/0000-0001-6201-3251
Wei Tu http://orcid.org/0000-0002-4749-6037
Rui Cao http://orcid.org/0000-0002-1440-4175
Qili Gao http://orcid.org/0000-0003-0179-3500
Guanzhou Chen http://orcid.org/0000-0003-0733-9122

Data availability statement

Building and POI data are accessible from GaoDe, a digital map service of China, and mobile phone data are available from Smartsteps; there are constraints on the availability of these data, which were utilized under permission for the current study and are thus not publicly available. Nonetheless, the data are available from the authors upon reasonable request and with the agreement of these organizations. OpenStreetMap (OSM) road network data are freely accessible at http://www.openstreetmap.org/, and GDP statistics have been publicly uploaded to the RESDC (https://www.resdc.cn/DOI/doi.aspx?DOIid=33).

References

Albert, R., and A.-L. Barabási. 2002. "Statistical Mechanics of Complex Networks." *Reviews of Modern Physics* 74 (1): 47–97. doi:10.1103/RevModPhys.74.47.

Arcaute, E., E. Hatna, P. Ferguson, H. Youn, A. Johansson, and M. Batty. 2015. "Constructing Cities, Deconstructing Scaling Laws." *Journal of the Royal Society Interface* 12 (102): 20140745. doi:10.1098/rsif.2014.0745.

Batty, M. 2008. "The Size, Scale, and Shape of Cities." *Science* 319 (5864): 769–771. doi:10.1126/science.1151419.

Becker, R., C. Volinsky, R. Cáceres, K. Hanson, S. Isaacman, J. M. Loh, M. Martonosi, J. Rowland, S. Urbanek, and A. Varshavsky. 2013. "Human Mobility Characterization from Cellular Network Data." *Communications of the ACM* 56 (1): 74. doi:10.1145/2398356.2398375.

Berry, B. J. L. 1964. "Cities as Systems Within Systems of Cities." *Papers of the Regional Science Association* 13 (1): 146–163. doi:10.1007/BF01942566.

Bettencourt, L. M. A. 2013. "The Origins of Scaling in Cities." *Science* 340 (6139): 1438–1441. doi:10.1126/science.1235823.

Bettencourt, L. M. A., and J. Lobo. 2016. "Urban Scaling in Europe." *Journal of the Royal Society Interface* 13 (116): 20160005. doi:10.1098/rsif.2016.0005.

Bettencourt, L. M. A., J. Lobo, D. Helbing, C. Kühnert, and G. B. West. 2007. "Growth, Innovation, Scaling, and the Pace of Life in Cities." *Proceedings of the National Academy of Sciences* 104 (17): 7301–7306. doi:10.1073/pnas.0610172104.

Bettencourt, L. M. A., J. Lobo, and H. Youn. 2013. "The Hypothesis of Urban Scaling: Formalization, Implications and Challenges." *ArXiv:1301.5919 [Nlin, Physics:Physics]*, January. Accessed 12 July 2019. http://arxiv.org/abs/1301.5919

Bettencourt, L. M. A., and G. B. West. 2011. "Bigger Cities Do More with Less." *Scientific American* 305 (3): 52–53. doi:10.1038/scientificamerican0911-52.

Blondel, V. D., A. Decuyper, and G. Krings. 2015. "A Survey of Results on Mobile Phone Datasets Analysis." *EPJ Data Science* 4 (1): 10. doi:10.1140/epjds/s13688-015-0046-0.

Bokányi, E., Z. Kallus, and I. Gódor. 2019. "Collective Sensing of Evolving Urban Structures: From Activity-Based to Content-Aware Social Monitoring." *Environment and Planning B: Urban Analytics and City Science* 48 (1): 239980831984876, May. doi:10.1177/2399808319848760.

Brockmann, D., L. Hufnagel, and T. Geisel. 2006. "The Scaling Laws of Human Travel." *Nature* 439 (7075): 462–465. doi:10.1038/nature04292.

Calabrese, F., G. Di Lorenzo, L. Liu, and C. Ratti. 2011. "Estimating Origin-Destination Flows Using Mobile Phone Location Data." *IEEE Pervasive Computing* 10 (4): 36–44. doi:10.1109/MPRV.2011.41.

Calabrese, F., Z. Smoreda, V. D. Blondel, and C. Ratti. 2011. "Interplay Between Telecommunications and Face-To-Face Interactions: A Study Using Mobile Phone Data." *Plos One* 6 (7): e20814. doi:10.1371/journal.pone.0020814.

Cao, J., Q. Li, W. Tu, Q. Gao, R. Cao, and C. Zhong. 2021. "Resolving Urban Mobility Networks from Individual Travel Graphs Using Massive-Scale Mobile Phone Tracking Data." *Cities* 110 (March): 103077. doi:10.1016/j.cities.2020.103077.

Cao, J., Q. Li, W. Tu, and F. Wang. 2019. "Characterizing Preferred Motif Choices and Distance Impacts." *Plos One* 14 (4): e0215242. doi:10.1371/journal.pone.0215242.

Cavoli, C. 2021. "Accelerating Sustainable Mobility and Land-Use Transitions in Rapidly Growing Cities: Identifying Common Patterns and Enabling Factors." *Journal of Transport Geography* 94 (June): 103093. doi:10.1016/j.jtrangeo.2021.103093.

Cesaretti, R., J. Lobo, L. M. A. Bettencourt, S. G. Ortman, and M. E. Smith. 2016. "Population-Area Relationship for Medieval European Cities." *Plos One* 11 (10): e0162678. doi:10.1371/journal.pone.0162678.

Chong, M., A. Habib, N. Evangelopoulos, and H. W. Park. 2018. "Dynamic Capabilities of a Smart City: An Innovative Approach to Discovering Urban Problems and Solutions." *Government Information Quarterly* 35 (4): 682–692, August. doi:10.1016/j.giq.2018.07.005.

"Communiqué of the Seventh National Census of Shenzhen." 2021. May. http://tjj.sz.gov.cn/ztzl/zt/szsdqcqgrkpc/

D'Silva, K., A. Noulas, M. Musolesi, C. Mascolo, and M. Sklar. 2018. "Predicting the Temporal Activity Patterns of New Venues." *EPJ Data Science* 7 (1): 13. doi:10.1140/epjds/s13688-018-0142-z.

Deville, P., C. Linard, S. Martin, M. Gilbert, F. R. Stevens, A. E. Gaughan, V. D. Blondel, and A. J. Tatem. 2014. "Dynamic Population Mapping Using Mobile Phone Data." *Proceedings of the National Academy of Sciences of the United States of America* 111 (45): 15888–15893. doi:10.1073/pnas.1408439111.

Diao, M., H. Kong, and J. Zhao. 2021. "Impacts of Transportation Network Companies on Urban Mobility." *Nature Sustainability*, February 1–7. doi:10.1038/s41893-020-00678-z.

Dong, L., Z. Huang, J. Zhang, and Y. Liu. 2020. "Understanding the Mesoscopic Scaling Patterns Within Cities." *Scientific Reports* 10 (1): 21201. doi:10.1038/s41598-020-78135-2.

Dorogovtsev, S. N., A. V. Goltsev, and J. F. F. Mendes. 2002. "Pseudofractal Scale-Free Web." *Physical Review E* 65 (6): 066122. doi:10.1103/PhysRevE.65.066122.

Eeckhout, J. 2004. "Gibrat's Law for (All) Cities." *The American Economic Review* 94 (5): 1429–1451. doi:10.1257/0002828043052303.

Gallotti, R., and M. Barthelemy. 2014. "Anatomy and Efficiency of Urban Multimodal Mobility." *Scientific Reports* 4 (November): srep06911. doi:10.1038/srep06911.

Gao, Q., Y. Yue, W. Tu, J. Cao, and Q. Li. 2021. "Segregation or Integration? Exploring Activity Disparities Between Migrants and Settled Urban Residents Using Human Mobility Data." *Transactions in GIS* 25 (6): 2791–2820. doi:10.1111/tgis.12760.

Giometto, A., F. Altermatt, F. Carrara, A. Maritan, and A. Rinaldo. 2013. "Scaling Body Size Fluctuations." *Proceedings of the National Academy of Sciences* 110 (12): 4646–4650. doi:10.1073/pnas.1301552110.

Gong, J., and G. Xu. 2021. "Urban Scaling Law and Its Application." *Acta Geographica Sinica* 76 (2): 251–260. doi:10.11821/dlxb202102001.

Guidotti, R., A. Monreale, S. Rinzivillo, D. Pedreschi, and F. Giannotti. 2016. "Unveiling Mobility Complexity Through Complex Network Analysis." *Social Network Analysis and Mining* 6 (1): 59. doi:10.1007/s13278-016-0369-2.

Hoteit, S., S. Secci, S. Sobolevsky, C. Ratti, and G. Pujolle. 2014. "Estimating Human Trajectories and Hotspots Through Mobile Phone Data." *Computer Networks* 64 (May): 296–307. doi:10.1016/j.comnet.2014.02.011.

Huang, J., D. Levinson, J. Wang, J. Zhou, and Z. Wang. 2018. "Tracking Job and Housing Dynamics with Smartcard Data." *Proceedings of the National Academy of Sciences* 115 (50): 12710–12715. doi:10.1073/pnas.1815928115.

Jiao, L., W. Lei, G. Xu, Z. Xu, and Z. Zhou. 2021. "Urban Scaling and the Spatio-Temporal Characteristics of Scaling Exponents in China." *Acta Geographica Sinica* 75 (12): 2744–2758. doi:10.11821/dlxb202012014.

Kleiber, M. 1947. "Body Size and Metabolic Rate." *Physiological Reviews* 27 (4): 511–541. doi:10.1152/physrev.1947.27.4.511.

Kühnert, C., D. Helbing, and G. B. West. 2006. "Scaling Laws in Urban Supply Networks." *Physica A: Statistical Mechanics and Its Applications* 363 (1): 96–103. doi:10.1016/j.physa.2006.01.058.

Lei, W., L. Jiao, Z. Xu, Z. Zhou, and G. Xu. 2021. "Scaling of Urban Economic Outputs: Insights Both from Urban Population Size and Population Mobility." *Computers, Environment and Urban Systems* 88 (July): 101657. doi:10.1016/j.compenvurbsys.2021.101657.

Liang, X., J. Zhao, L. Dong, and K. Xu. 2013. "Unraveling the Origin of Exponential Law in Intra-Urban Human Mobility." *Scientific Reports* 3 (October). doi:10.1038/srep02983.

Liu, X., N. Niu, X. Liu, H. Jin, J. Ou, L. Jiao, and Y. Liu. 2018. "Characterizing Mixed-Use Buildings Based on Multi-Source Big Data." *International Journal of*

Geographical Information Science 32 (4): 738–756. doi:10.1080/13658816.2017.1410549.

Longley, P. A. 2017. "Modifiable Areal Unit Problem." In *International Encyclopedia of Geography*, 1–4. American Cancer Society. doi:10.1002/9781118786352.wbieg0344.

Louail, T., M. Lenormand, O. G. Cantu Ros, M. Picornell, R. Herranz, E. Frias-Martinez, J. J. Ramasco, and M. Barthelemy. 2015. "From Mobile Phone Data to the Spatial Structure of Cities." *Scientific Reports* 4 (1): 5276. doi:10.1038/srep05276.

Maeda, T. N., N. Shiode, C. Zhong, J. Mori, and T. Sakimoto. 2019. "Detecting and Understanding Urban Changes Through Decomposing the Numbers of Visitors' Arrivals Using Human Mobility Data." *Journal of Big Data* 6 (1): 4. doi:10.1186/s40537-019-0168-5.

Meirelles, J., C. R. Neto, F. F. Ferreira, F. L. Ribeiro, and C. R. Binder. 2018. "Evolution of Urban Scaling: Evidence from Brazil." Edited by Celine Rozenblat. *Plos One* 13 (10): e0204574. doi:10.1371/journal.pone.0204574.

Meirelles, J., F. L. Ribeiro, G. Cury, C. R. Binder, and V. M. Netto. 2021. "More from Less? Environmental Rebound Effects of City Size." *Sustainability* 13 (7): 4028. doi:10.3390/su13074028.

Niu, N., X. Liu, H. Jin, X. Ye, Y. Liu, X. Li, Y. Chen, and S. Li. 2017. "Integrating Multi-Source Big Data to Infer Building Functions." *International Journal of Geographical Information Science* 31 (9): 1871–1890. doi:10.1080/13658816.2017.1325489.

Norman, J., H. L. MacLean, and C. A. Kennedy. 2006. "Comparing High and Low Residential Density: Life-Cycle Analysis of Energy Use and Greenhouse Gas Emissions." *Journal of Urban Planning and Development* 132 (1): 10–21. doi:10.1061/(ASCE)0733-9488(2006)132:1(10).

Ravasz, E., and A.-L. Barabási. 2003. "Hierarchical Organization in Complex Networks." *Physical Review E* 67 (2): 026112. doi:10.1103/PhysRevE.67.026112.

Ribeiro, H. V., M. Oehlers, A. I. Moreno-Monroy, J. P. Kropp, and D. Rybski. 2021. "Association Between Population Distribution and Urban GDP Scaling." *Plos One* 16 (1): e0245771. doi:10.1371/journal.pone.0245771.

Rozenfeld, H. D., D. Rybski, J. S. Andrade, M. Batty, H. E. Stanley, and H. A. Makse. 2008. "Laws of Population Growth." *Proceedings of the National Academy of Sciences* 105 (48): 18702–18707. doi:10.1073/pnas.0807435105.

Rybski, D., E. Arcaute, and M. Batty. 2019. "Urban Scaling Laws." *Environment and Planning B: Urban Analytics and City Science* 46 (9): 1605–1610. doi:10.1177/2399808319886125.

Rybski, D., S. V. Buldyrev, S. Havlin, F. Liljeros, and H. A. Makse. 2009. "Scaling Laws of Human Interaction Activity." *Proceedings of the National Academy of Sciences* 106 (31): 12640–12645. doi:10.1073/pnas.0902667106.

Sahasranaman, A., and L. M. A. Bettencourt. 2019. "Urban Geography and Scaling of Contemporary Indian Cities." *Journal of the Royal Society Interface* 16 (152): 20180758. doi:10.1098/rsif.2018.0758.

Schläpfer, M., L. Dong, K. O'Keeffe, P. Santi, M. Szell, H. Salat, S. Anklesaria, M. Vazifeh, C. Ratti, and G. B. West. 2021. "The Universal Visitation Law of Human Mobility." *Nature* 593 (7860): 522–527. doi:10.1038/s41586-021-03480-9.

Strano, E., A. Giometto, S. Shai, E. Bertuzzo, P. J. Mucha, and A. Rinaldo. 2017. "The Scaling Structure of the Global Road Network." *Open Science* 4 (10): 170590. doi:10.1098/rsos.170590.

Thatcher, J., A. Shears, and J. Eckert. 2018. "Thinking Big Data in Geography: New Regimes, New Research." https://digitalcommons.tacoma.uw.edu/urban_books/25

Tu, W., J. Cao, Y. Yue, S.-L. Shaw, M. Zhou, Z. Wang, X. Chang, Y. Xu, and Q. Li. 2017. "Coupling Mobile Phone and Social Media Data: A New Approach to Understanding Urban Functions and Diurnal Patterns." *International Journal of Geographical Information Science* 31 (12): 2331–2358. doi:10.1080/13658816.2017.1356464.

Tu, W., R. Cao, Y. Yue, B. Zhou, Q. Li, and Q. Li. 2018. "Spatial Variations in Urban Public Ridership Derived from GPS Trajectories and Smart Card Data." *Journal of Transport Geography* 69 (May): 45–57. doi:10.1016/j.jtrangeo.2018.04.013.

Tu, W., T. Zhu, J. Xia, Y. Zhou, Y. Lai, J. Jiang, and Q. Li. 2020. "Portraying the Spatial Dynamics of Urban Vibrancy Using Multisource Urban Big Data." *Computers, Environment and Urban Systems* 80 (March): 101428. doi:10.1016/j.compenvurbsys.2019.101428.

Wang, W., L. Pan, N. Yuan, S. Zhang, and D. Liu. 2015. "A Comparative Analysis of Intra-City Human Mobility by Taxi." *Physica A: Statistical Mechanics and Its Applications* 420 (February): 134–147. doi:10.1016/j.physa.2014.10.085.

Xu, X. 2017. "China GDP Spatial Distribution Kilometer Grid Dataset." *Data Registration and Publishing System of the Resource and Environmental Science Data Center of the Chinese Academy of Sciences*. doi:10.12078/2017121102

Xu, Y., A. Belyi, I. Bojic, and C. Ratti. 2018. "Human Mobility and Socioeconomic Status: Analysis of Singapore and Boston." *Computers, Environment and Urban Systems* 72 (November): 51–67. doi:10.1016/j.compenvurbsys.2018.04.001.

Xu, G., Z. Zhou, L. Jiao, T. Dong, and R. Li. 2019. "Cross-Sectional Urban Scaling Fails in Predicting Temporal Growth of Cities." *ArXiv:1910.06732 [Physics]*, October. Accessed 2 August 2020. http://arxiv.org/abs/1910.06732

Yan, X., X.-P. Han, B. Wang, and T. Zhou. 2013. "Diversity of Individual Mobility Patterns and Emergence of Aggregated Scaling Laws." *Scientific Reports* 3 (September): 2678. doi:10.1038/srep02678.

Yin, J., and G. Chi. 2021. "Characterizing People's Daily Activity Patterns in the Urban Environment: A Mobility Network Approach with Geographic Context-Aware Twitter Data." *Annals of the American Association of Geographers* 1–21. doi:10.1080/24694452.2020.1867498.

Zheng, Z., and S. Zhou. 2017. "Scaling Laws of Spatial Visitation Frequency: Applications for Trip Frequency Prediction." *Computers, Environment and Urban Systems* 64 (July): 332–343. doi:10.1016/j.compenvurbsys.2017.04.004.

Zhou, Y., R. Xu, D. Hu, Y. Yue, Q. Li, and J. Xia. 2020. "Effects of Human Mobility Restrictions on the Spread of COVID-19 in Shenzhen, China: A Modelling Study Using Mobile Phone Data." *Lancet Digital Health* 2 (8): e417–24. doi:10.1016/S2589-7500(20)30165-5.

Zhou, X., A. G. O. Yeh, and Y. Yue. 2018. "Spatial Variation of Self-Containment and Jobs-Housing Balance in Shenzhen Using Cellphone Big Data." *Journal of Transport Geography* 68 (April): 102–108. doi:10.1016/j.jtrangeo.2017.12.006.

Zünd, D., and L. M. A. Bettencourt. 2019. "Growth and Development in Prefecture-Level Cities in China." *Plos One* 14 (9): e0221017. doi:10.1371/journal.pone.0221017.